Journal of Materials Science: Materials in Electronics
https://doi.org/10.1007/s10854-019-01994-7

Improved quality of InP layer on GaAs substrates by using compositionally modulated step-graded AlGaInAs buffers

Yang He[1] · Wei Yan[2] · Yurun Sun[3] · Jianrong Dong[3]

Received: 26 April 2019 / Accepted: 4 August 2019

Abstract
Improved quality of metal–organic chemical vapor deposition grown InP layer on GaAs substrate was achieved by using compositional modulated step-graded $AlGaIn_xAs$ (x = 0.05–0.52) buffers. With the insertion of tensile stained AlGaInAs layers into the compressive buffers, we obtained a high crystal quality InP layer with a smooth surface and low threading dislocation confirmed by atomic force microscopy, transmission electron microscopy, photoluminescence and X-ray diffraction reciprocal space mapping. This indicated that the tensile strained AlGaInAs layers into the compressive AlGaInAs layers can change the glide direction and facilitate annihilation reactions of dislocations, and the interfaces also can prevent the vertical growth of threading dislocations propagating through the structures. The results show that the compositional modulated step-graded $AlGaIn_xAs$ buffers grown on GaAs hold great promise to be virtual substrates of other metamorphic devices.

1 Introduction

The manufacture of InP-based devices such as GaInAsP–InP lasers, GaInAs–InP photodetectors and InP solar cells on GaAs substrates is a new technique with many advantages, such as mechanical robustness, lower cost and wafer availability [1], however, ~ 3.8% large lattice mismatch will be introduced between GaAs and InP. The limitation of lattice constants on materials can be broken by growing metamorphic buffers, which has attracted much attention to favor the selection of appropriate materials for the metamorphic devices [2–4]. During the metamorphic buffers growth, the strain will be relieved by the dislocations as the buffer thickness exceeds the critical thickness. Once the threading dislocations (TDs) concomitantly generated with misfit dislocations (MDs) penetrate vertically through the buffers into the device active regions, they may be detrimental to optoelectronic devices acting as nonradiative recombination or scattering centers [4, 5]. On the one hand, an ideal metamorphic buffer should be attuned with the target device in the growing process, on the other hand it should promote the misfit dislocation glide along the interface while minimizing the threading dislocation nucleation to prevent the formation of TDs. Various schemes have been implemented to accomplish these goals, including a compositional step-graded [6, 7], linearly-graded [8, 9] or reverse-graded buffers [10–12], and overshoot [13] or reverse steps [14] on the top layer and so on. Especially, the compositional gradients structures have been demonstrated to diminish the densities of TD (TDDs) proficiently because of the interfaces created between the contiguous steps. Metamorphic $AlGaIn_xAs$ buffers with lattice parameter overlying from GaAs to InP can be developed on GaAs, Ge, or InP substrates to attain the objective lattice conversion.

In our work, a compositional modulated step-graded $AlGaIn_xAs$ (x = 0.05–0.52) buffer was employed between GaAs substrate and InP cap layer. Different from the common metamorphic buffer growth, we inserted some reverse tensile step-graded AlGaInAs buffers into the common step-graded AlGaInAs with compression strain. The experiment results show that the compositional modulated step-graded AlGaInAs buffers can improve the crystal quality of InP cap layer, that is to say, smooth the surface morphology and reduce the TDDs of InP. In comparation with more usual

✉ Yang He
yhe2013@sinano.ac.cn

[1] School of Electronic Engineering, Changzhou College of Information Technology, No. 22 Middle Mingxin Road, Wujin District, Changzhou 213164, China

[2] Basic Courses Department, Changzhou College of Information Technology, No. 22 Middle Mingxin Road, Wujin District, Changzhou 213164, China

[3] Key Laboratory of Nano Devices and Applications, Suzhou Institute of Nano-Tech and Nano-Bionics, Chinese Academy of Sciences (CAS), Suzhou 215123, China

Published online: 08 August 2019

compositional monotonically step-graded buffer, the application of compositional non-monotonically step-graded buffer provides various options for enlarging the growth strategy of metamorphic buffers to overcome the lattice mismatch.

2 Experiment

The two samples under investigation were grown in a horizontal low-pressure (10^4 pa) metal–organic chemical vapor deposition (MOCVD) system on (001)-oritented n-doped GaAs substrate with 15° misorientation toward (111)A, using trimethylallium (TMGa), trimethylindium (TMIn), trimethylaluminum (TMAl), phosphide (PH_3) and arsenide hydrogen (AsH_3) as precursors, and ultra high purity hydrogen (H_2) was used as the carrier gas. An initial 100 nm thick GaAs layer was deposited in order to obtain a smooth epilayer. After GaAs growth, a $AlGaIn_xAs$ (x = 0.05–0.52) buffer was developed at a nominal rate of ~ 0.67 nm/s and at an unbroken inside growth chamber of 700 °C under adjusting the Al, Ga, and In compositions to meet the band gap of AlGaInAs buffers at ~ 1.5 eV. Both monotonically step-graded (sample A) and non-monotonically step-graded (sample B) structures were grown, for the latter one, in which the indium content undulates to get alternate growth of compressive strain and tensile strain materials, i.e. a low In content follows a high In content and is followed by a higher In content again,as exhibited in Fig. 1. In the two samples, the aggregate thickness of AlGaInAs buffers is the same and after that, InP layer was grown. The only different between the two samples is that ten 100 nm thick reverse-graded AlGaInAs intermediate layers were inserted into ten step-graded buffers with 180 nm for sample B, and each of the AlGaInAs layer was 280 nm thick instead for sample A.

Multiple techniques were used to analyze the quality of the two metamorphic structures. The Veeco Dimension 3100 atomic force microscopy (AFM) with the Nanoscope IIId controller in tapping mode was employed to examine the surface morphology and root-mean-square (RMS) roughness. The photoluminescence (PL) were performed to investigate the quality of InP by a mapping system (RPM 2000) with a 532 nm excitation laser. The samples were imaged with a JOE-2000 transmission electron microscope (TEM) working operated at 200 kV to evaluate the crystal microstructures and dislocation distributions.

3 Discussion and results

The room PL spectra emitted from InP cap layer of samples A and B given in Fig. 2. It shows that the PL peak is at about 912.5 nm, however, the PL peak intensity is much smaller and the full width at half maximum (FWHM) is larger for sample A than those of sample B, specifying much more TDs as nonradiative recombination centers been in the top layer of sample A. The TEM analysis is employed to get further insight into the structural properties of the both AlGaInAs buffers. Figure 3a displays a cross-sectional TEM (XTEM) image of sample A grown using conventional step-graded buffers. The first six layers contain much higher threading dislocation densities (TDDs), however, in the other AlGaInAs buffers, most of the misfit dislocations are restricted near the internal interface, which is related to a larger value of FWHM along the q_x direction in the images of RSMs. Figure 3b shows one sample grown using compositional modulated step-graded buffers (sample B). Misfit

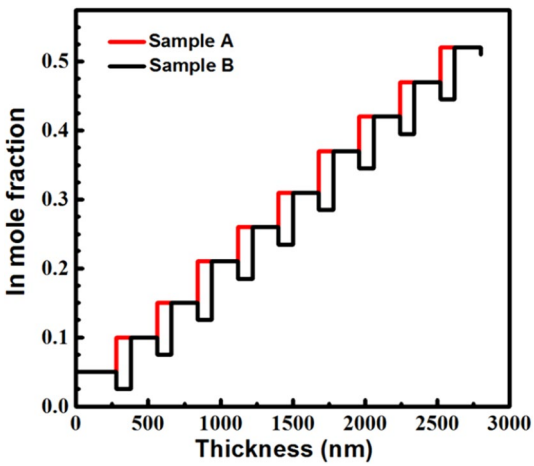

Fig. 1 Schematic diagrams of buffer structures for sample A and sample B. In the metamorphic buffers of sample A, the In component was increased monotonically by steps. In that of sample B, tensile AlGaInAs layers were inserted between the compressive AlGaInAs layers

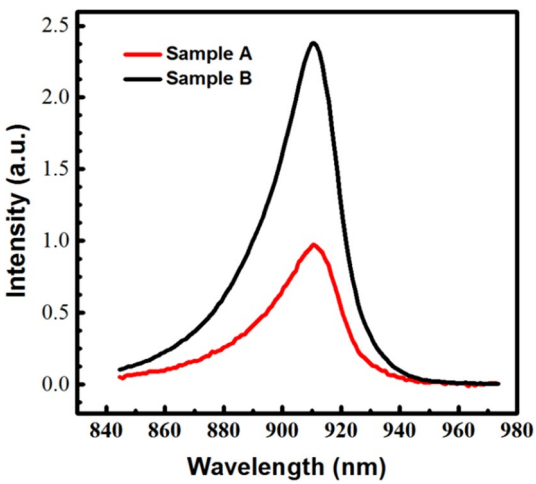

Fig. 2 Photoluminescence spectra of InP cap layers of samples A and B measured at room temperature

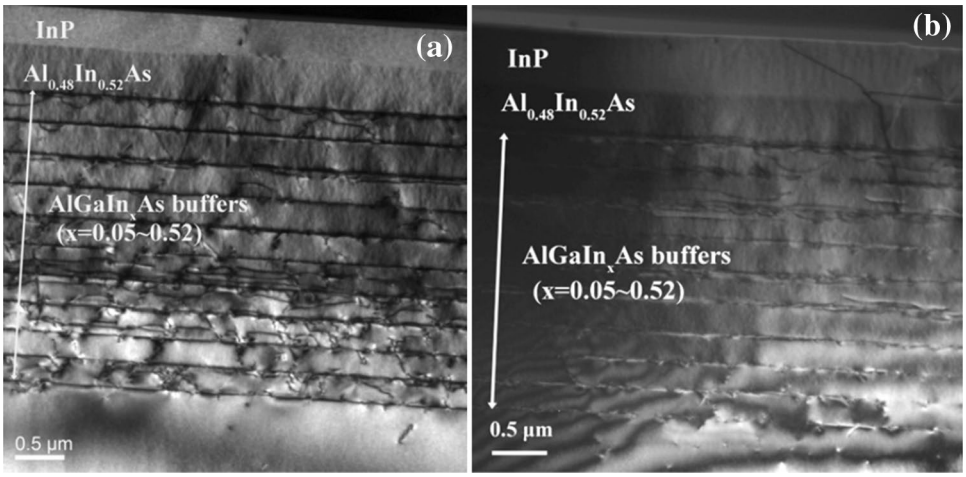

Fig. 3 XTEM microscopy of **a** sample A and **b** B with the diffraction vector g = <220>

dislocations are limited along the internal interfaces and few propagate upright throughout the structures. The dislocation located at internal interfaces serves to significantly decrease TDs in the last $Al_{0.48}In_{0.52}As$ and InP layer, which explains the reduction of the FWHM in the q_x direction compared to the sample grown by the first method (sample A). The XTEM results demonstrate the high material quality of InP grown on GaAs substrate using compositional modulated step-graded AlGaIn$_x$As buffers and attest the high efficiency of compositional modulated step-graded AlGaIn$_x$As buffers to inhibit migration of TDs in the strain relaxation process.

The assessment of the stain relaxation in the InP/AlGaInAs metamorphic buffers were made according to the measurements of reciprocal space mappings (RSMs) with symmetric (004) and asymmetric (224) reflections by using a high resolution X-ray diffractometer (HRXRD). Figure 4 exhibits the RSMs of (224) planes of samples A and B with the incident X-ray beam along the [110] direction. The vertical and horizontal axes signify the reciprocal lattice of the [001] (Q_z) and [110] (Q_x) directions, respectively. In each figure, the GaAs substrate, the AlGaInAs (x = 0.05–0.52) buffers and InP top layer are well distinguished. The In component and the strain relaxation ratio of each metamorphic AlGaIn$_x$As buffers is calculated from the diffraction peak position relative to the GaAs substrate peak, modified using the epilayer tilting effect exhibited in the (004) RSMs image (Fig. 5). The RSMs from the symmetric reflection determine the out-of-plane lattice parameter $a_\perp$ perpendicular to the (001) surface and the RSMs from the asymmetric reflection determine the in-plane lattice parameters $a_{[110]}$ and $a_{[1-10]}$, respectively. The out-of-plane lattice parameter in the [001] direction from the symmetric (004) RSM can be simply given by:

$$a_\perp = \frac{4}{\left(4/a_{sub}\right) - \left|\Delta Q_Z^{004}\right|} \tag{1}$$

while the in-plane lattice parameter along the orthogonal <110> directions can be calculated from:

$$a_{110} = \frac{2\sqrt{2}}{\left(2\sqrt{2}/a_{sub}\right) - \left|\Delta Q_x^{224}\right|} \tag{2}$$

where ΔQ_x^{224} is the tilt-corrected peak splitting between the InP cap layer and substrate in each <110> directions. The lattice constant of fully relaxed epilayer can be determined by:

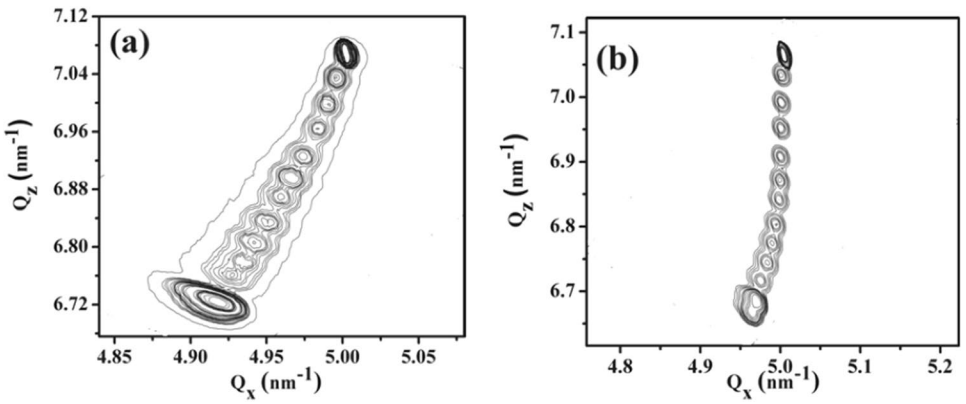

Fig. 4 Asymmetric (224) RSMs of samples A (**a**) and B (**b**) with projection of the incident beam on (001) surface along the [110] direction

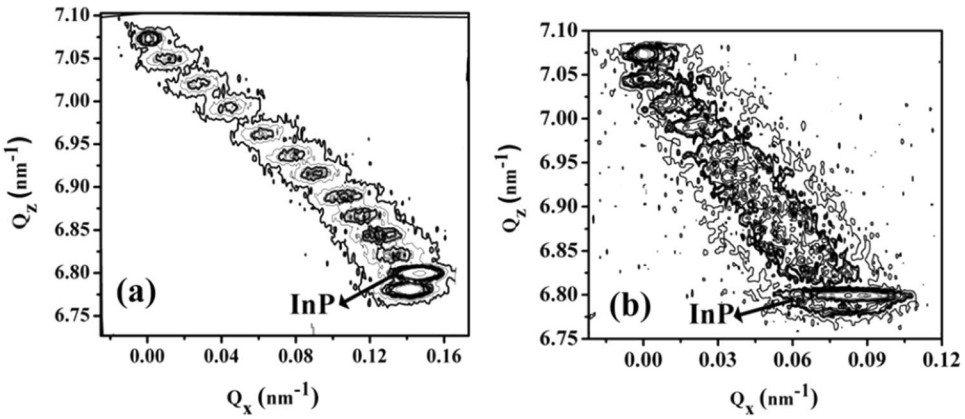

Fig. 5 Symmetric (004) RSMs of samples A (**a**) and B (**b**) with projection of the incident beam on (001) surface along the [110] direction

Table 1 Stain relaxation rate of samples A and B alongthe [110] and [1−10] directions

Sample	Strain relaxation rate (%)	
	[110]	[1−10]
A	96.7	95.2
B	98.3	97.6

Table 2 Four slip systems of α dislocations for the epilayer of (001) zinc-blend semiconductors

System	Line vector	Glide plane	Burgers vector
S1	1/2a[1–10]	(111)	1/2a[10−1]
S2	1/2a[1–10]	(111)	1/2a[01−1]
S3	1/2a[1–10]	(−1−11)	1/2a[101]
S4	1/2a[1–10]	(−1−11)	1/2a[011]

$$a_0 = \frac{1-\nu}{1+\nu}a_{\perp} + \frac{\nu}{1+\nu}\left(a_{[110]} + a_{[1-10]}\right) \tag{3}$$

where υ is the Poisson ratio and then the strain relaxation degree in each <110> direction can be expressed by:

$$R_{110} = \frac{a_{110} - a_{sub}}{a_0 - a_{sub}} \tag{4}$$

In consequence, from the formulas above we can get the strain relaxation rate is about 96.7% in the [110] direction and 95.2% in the [1−10] direction for sample A, while 98.3% in the [110] direction and 97.6% in the [1−10] direction as shown in Table 1, respectively. The strain relaxation results of both samples demonstrated that the TDDs reduction of sample B is not resulted from the difference of relieved strain, but the lower TDDs in sample B is sufficiently related with the buffer structures between the InP cap layer and GaAs substrate. The layer strain relaxations of InP by two different growth methods are almost the same, however, the diffraction peaks of the AlGaInAs metamorphic buffers show obvious difference. In Fig. 4a, the mosaic perpendicular to the scattering vector of sample A is more broadening than that of sample B, indicating the broadening of the peak of RSMs is caused by different sources of crystal imperfections [15] and sample A has a higher TDDs in the AlGaInAs metamorphic buffers than that of sample B, which is accordance with the TEM and PL results.

In the (004) RSMs of samples A and B with the incident X-ray beam along the [110] direction indicated in Fig. 5, the diffraction intensity maximum for the epilayer and substrate is split, representing the tilt exited with respect to the substrate [16]. Obviously, the tilt was generated between the InP layer and GaAs substrate, normally about 1.22° for conventional step-graded buffers (sample A) and 0.67° for modulated compositional step-graded buffers (sample B). In zinc blend semiconductors, α-type and β-type dislocations, whose line vector is along the [1−10] and [110] directions, respectively [17], are generated to relieve the compressive misfit strain. For a (001) epilayer, α dislocations glide on the four 1/2a <110> {111} slip systems as shown in Table 2. These burger vectors can be resolved into three components given in Fig. 6 and ideally these components will cancel each other and no net tilt will be generated if the α dislocation nucleation between the (111) and (−1−11) planes is sufficiently random and isotropic, otherwise, a tilt would be produced. Consequently, the tilt generated along the [110] direction in samples A and B implies an imbalance distribution of α dislocations in both planes. The tilt of sample B is smaller than that of sample A, indicating that the insertion of tensile-strained AlGaInAs layer can balance the uneven misfit strain distribution at different slip planes and facilitate the α dislocation distribution equally, which is helpful to promote dislocation gliding and decrease the TDDs. Ultimately, α dislocation density in the compositional modulated step-graded buffers (sample B) is smaller than that of conventional buffers (sample A), which will also be proved in the below.

During the lattice relaxation process of metamorphic AlGaInAs buffers, α dislocations are firstly nucleated due to their low nucleation energy compared with β dislocations.

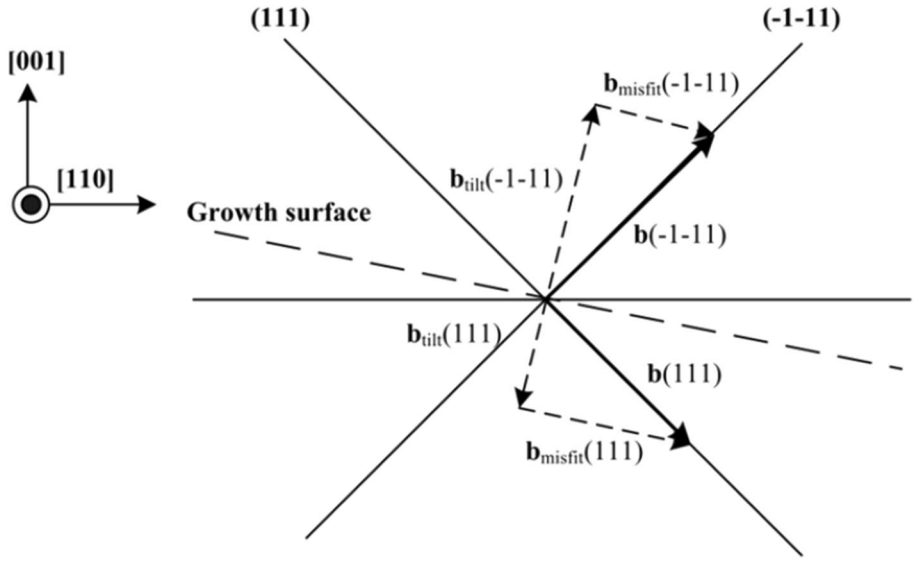

Fig. 6 Illustration of the asymmetry in misfit components at the growth surface between the (111) and (−1−11) planes on a (001) substrate with a miscut toward (111)A

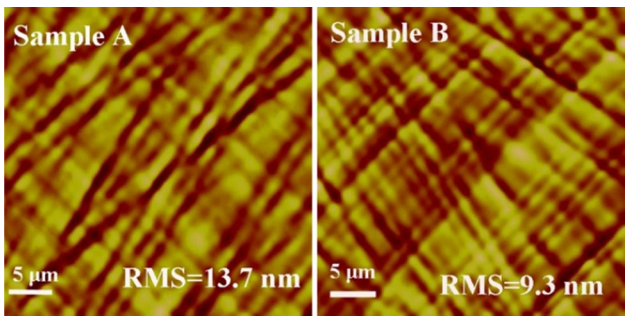

Fig. 7 AFM images of samples A and B with scan area of 40 μm×40 μm

It has reported that the large miscut toward (111)A can make α dislocations parallel along the [1−10] directions while the β dislocations will cross over with each other in their slip planes [18], and that the β dislocations gliding will be blocked by the strong wall of strain field built by parallel-distributed α dislocations [19]. For sample B, the insertion of tensile stained buffers can change the dislocations gliding direction and can reduce α dislocations, weakening the negative effects of α dislocations on the β dislocations gliding and the α dislocations reduction can decrease the β dislocations.

As seen from Fig. 7, the sample B grown under the optimized conditions has the smallest RMS value of 9.3 nm compared with the 13.7 nm of sample A, indicating the insertion of the reverse-graded AlGaInAs buffers smoothes the surface roughness significantly. The tensile AlGaInAs layers reduce the surface strain fluctuations to make the strain field equally distributed. In the process of epitaxial layer growth, the surface atoms tend to diffuse at the appropriate sites to smooth the surface. In turn, the smooth surface leads to a lower possibility to prevent the dislocations gliding vertically into the upper layer [19]. But beyond the discussion above, the reverse tensile AlGaInAs buffers actually increase the annihilation probability of dislocation interactions. As shown in the XTEM images, most of defects are confined along the interface of sample B. In the AlGaInAs metamorphic buffers, the compressive stain was not relieved sufficiently at the initial stage, while the small tensile strain plays an important role in improving the surface morphology by decreasing the surface strain fluctuations and then facilitated dislocations to glide along the interface and relax the residual strain. On the other hand, during the strain relaxation process in the metamorphic buffers, the dislocation line direction will rotate 90° from the compressive stress field to tensile stress field, and the dislocation glide direction does alter simultaneously. Eventually, the change of dislocation glide at the interfaces between the compressive and tensile AlGaInAs in the sample B enhances the dislocation annihilation to reduce the TDDs, which is consistence with our experiement results above.

4 Conclusions

In this paper, the InP cap layer with 3.8% lattice mismatch to GaAs substrate have been grown by MOCVD using different growth strategy, and the threading dislocation densities are reduced by using compositional modulated step-graded AlGaInAs buffers. In sample B, the insertion of tensile AlGaInAs layers changing the strain around the interface significantly reduces the threading dislocation density in InP cap layer by changing the dislocation glide direction and facilitating the dislocation annihilation reactions, and the interfaces also prevent the threading dislocations from

propagating vertically through the structure. Therefore, the compositional modulated AlGaInAs step-graded buffers can be very effective to control the threading dislocations and provide a new growth strategy to break the limitation of lattice constants on materials for the achievement of desired metamorphic devices.

Acknowledgements This work was supported by the University-level scientific research projects of Changzhou College of Information Technology [Grant No. CXZK201806Q] and the CCIT Key Laboratory of Industrial IoT (KYPT201803Z).

References

1. P. Merken et al., Extended-wavelength InGaAs-on-GaAs infrared focal-plane array. Electron. Lett. **38**, 588 (2002)
2. A.Y. Kim, M.E. Groenert, E.A. Fitzgerald, Visible light-emitting diodes grown on optimized ∇ x [In x Ga 1 − x]P/GaP epitaxial transparent substrates with controlled dislocation density. J. Electron. Mater. **29**, L9 (2000)
3. H.Q. Zheng et al., Metamorphic InP/InGaAs double-heterojunction bipolar transistors on GaAs grown by molecular-beam epitaxy. Appl. Phys. Lett. **77**, 869 (2000)
4. C.L. Andre et al., Investigations of high-performance GaAs solar cells grown on Ge-Si1-xGex-Si substrates. IEEE Trans. Electron Devices **52**, 1055 (2005)
5. C.L. Andre et al., Impact of dislocation densities on n+/p and p+/n junction GaAs diodes and solar cells on SiGe virtual substrates. J. Appl. Phys. **98**, 3884 (2005)
6. M.K. Hudait et al., 0.6-eV bandgap In/sub 0.69/Ga/sub 0.31/As thermophotovoltaic devices grown on InAs/sub y/P/sub 1-y/step-graded buffers by molecular beam epitaxy. Electron Device Lett. IEEE **24**, 538 (2003)
7. T. Sato, M. Akabori, S. Yamada, High-quality highly mismatched InSb films grown on GaAs substrate via thick AlSb and In x Al 1–x Sb step-graded buffers. Physica E **21**, 615 (2004)
8. K. Yuan et al., Characterization of linearly graded metamorphic InGaP buffer layers on GaAs using high-resolution X-ray diffraction. Thin Solid Films **391**, 36 (2001)
9. J.A. Olsen et al., Strain relaxation and surface roughness as a function of growth temperature in linearly graded InxAl1-xAs (x = 0.05 to 0.25) buffers. MRS Proc. (1993). https://doi.org/10.1557/PROC-326-395
10. B. Lee et al., Optical properties of InGaAs linear graded buffer layers on GaAs grown by metalorganic chemical vapor deposition. Appl. Phys. Lett. **68**, 2973 (1996)
11. J. Kirch et al., InAs y P 1 − y metamorphic buffer layers on InP substrates for mid-IR diode lasers. J. Cryst. Growth **312**, 1165 (2009)
12. V.A. Shah et al., Reverse graded SiGe/Ge/Si buffers for high-composition virtual substrates. J. Appl. Phys. **107**, R75 (2010)
13. J. Tersoff, Dislocations and strain relief in compositionally graded layers. Appl. Phys. Lett. **64**, 2748 (1994)
14. L.H. Wong et al., Strain relaxation mechanism in a reverse compositionally graded SiGe heterostructure. Appl. Phys. Lett. **90**, 460 (2007)
15. L. Hai et al., X-ray diffraction analysis of step-graded In x Ga 1–x As buffer layers grown by molecular beam epitaxy. J. Cryst. Growth **323**, 17 (2011)
16. R.S. Goldman et al., Effects of GaAs substrate misorientation on strain relaxation in InxGa1 − xAs films and multilayers. J. Appl. Phys. **83**, 5137 (1998)
17. R.S. Goldman et al., Effects of GaAs substrate misorientation on strain relaxation in InxGa1 − xAs films and multilayers. J. Appl. Phys. **83**, 5137 (1998)
18. F. Romanato et al., Strain relaxation in graded composition InxGa1 − xAs/GaAs buffer layers. J. Appl. Phys. **86**, 4748 (1999)
19. K.L. Li et al., Effects of substrate miscut on dislocation glide in metamorphic (Al)GaInP buffers. J. Cryst. Growth **380**, 261 (2013)